

1 **The influence of impactor size cut-off shift caused by hygroscopic growth**
2 **on particulate matter loading and composition measurements**

3 **Ying Chen^{1,2}, Oliver Wild¹, Yu Wang³, Liang Ran⁴, Monique Teich^{2,5}, Johannes Größ²,**
4 **Lina Wang^{2,5}, Gerald Spindler², Hartmut Herrmann², Dominik van Pinxteren², Gordon**
5 **McFiggans³ and Alfred Wiedensohler²**

6 ¹Lancaster Environment Centre, Lancaster University, Lancaster, LA1 4YQ, UK

7 ²Leibniz-Institute for Tropospheric Research, Leipzig, Germany

8 ³Centre for Atmospheric Sciences, School of Earth, Atmospheric and Environmental
9 Sciences, University of Manchester, Manchester, UK

10 ⁴Key Laboratory of Middle Atmosphere and Global Environment Observation, Institute of
11 Atmospheric Physics, Chinese Academy of Sciences, Beijing, China

12 ⁵Shanghai Key Laboratory of Atmospheric Particle Pollution and Prevention, Department of
13 Environmental Science and Engineering, Fudan University, Shanghai 200433, China

14 *Corresponding to: Ying Chen (y.chen65@lancaster.ac.uk)*

15
16 **Highlights:**

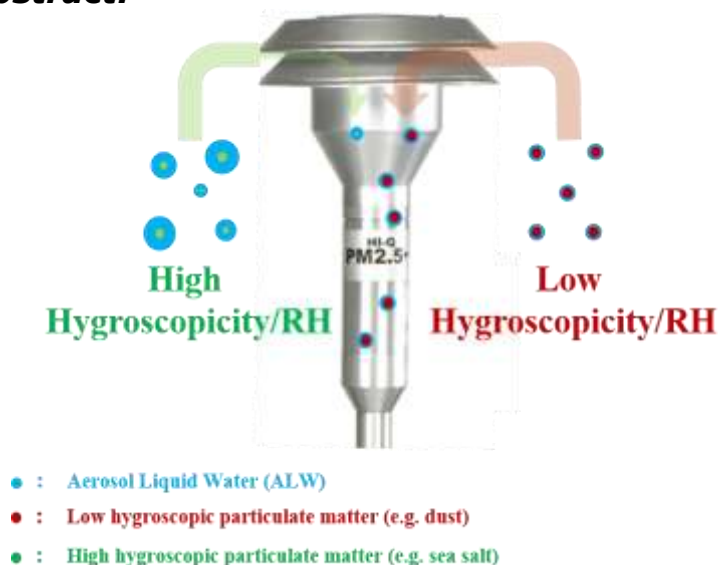
- 17 • Hygroscopic growth leads to a shift in the size of dry particles cut off by impactors used in
18 measurements of particle mass and composition.
- 19 • We propose a method for evaluating this influence on analysis of aerosol composition,
20 quantifying its global importance for the first time.
- 21 • Observational comparisons and model validation must account for the large temporal and
22 spatial variations in this influence.

24 **Abstract:**

25 The mass loading and composition of atmospheric particles are important in determining their
26 climate and health effects, and are typically measured by filter sampling. However, particle
27 sampling under ambient conditions can lead to a shift in the size cut-off threshold induced by
28 hygroscopic growth, and the influence of this on measurement of particle loading and
29 composition has not been adequately quantified. Here, we propose a method to assess this
30 influence based on κ -Köhler theory. A global perspective is presented based on previously
31 reported annual climatological values of hygroscopic properties, meteorological parameters
32 and particle volume size distributions. Measurements at background sites in Europe may be
33 more greatly influenced by the cut-off shift than those from other continents, with a median
34 influence of 10-20% on the total mass of sampled particles. However, the influence is generally
35 much smaller ($<7\%$) at urban sites, and is negligible for dust and particles in the Arctic. Sea-
36 salt particles experience the largest influence (median value $\sim 50\%$), resulting from their large
37 size, high hygroscopicity and the high relative humidity (RH) in marine air-masses. We
38 estimate a difference of $\sim 30\%$ in this influence of sea-salt particle sampling between relatively
39 dry (RH=60%) and humid (RH=90%) conditions. Given the variation in the cut-off shift in
40 different locations and at different times, a consistent consideration of this influence using the
41 approach we introduce here is critical for observational studies of the long-term and spatial
42 distribution of particle loading and composition, and crucial for robust validation of aerosol
43 modules in modelling studies.

44 **Keywords:** aerosol measurement; chemical composition; filter sampling; growth factor.

Graphical abstract:



45 **1. Introduction**

46 Particulate matter (PM) is currently of major concern around the world due to its effects on
47 human health (Meister et al., 2012; Pope et al., 2009) and climate change (IPCC, 2013;
48 Ramanathan & Carmichael, 2008; Seinfeld & Pandis, 2006). The mass loading and
49 composition of particles are crucial factors in these effects (Putaud et al., 2004; Seinfeld &
50 Pandis, 2006; Van Dingenen et al., 2004). Filter sampling and subsequent laboratory analysis
51 is one of the major ways to obtain particle composition and loading (Chow, 1995; Mader &
52 Pankow, 2001; Schaap et al., 2011). An impactor (or inlet head) is employed at the start of the
53 airflow to cut off particles larger than a certain size (Aufschnaiter, 2009; Berner & Luerzer,
54 1980; Marple et al., 1991; Schauer et al., 2003), so that PM₁, PM_{2.5} and PM₁₀ (particulate matter
55 with an aerodynamic diameter smaller than 1, 2.5 and 10 µm, respectively) can be collected on
56 filters for offline analysis. However, ambient particle diameter is strongly influenced by aerosol
57 liquid water (ALW), a ubiquitous and abundant aerosol constituent (Heintzenberg 1989; EPA
58 1999), whose amount is governed by particle hygroscopic growth. Global ALW may exceed
59 dry particle mass by a factor of more than two (Lee & Adams, 2010; Liao & Seinfeld, 2005;
60 Nguyen et al., 2016). Therefore, particle hygroscopic growth and ALW of ambient particles
61 can significantly influence the cut-off diameter of dry particles, and hence lead to a
62 considerable shift in the cut-off that impacts the particle composition and loading measured
63 using filter-based sampling.

64 The cut-off shift is determined by particle hygroscopicity, of which large variations have been
65 observed on a global scale (Liu et al., 2011; Nguyen et al., 2016; Pringle et al., 2010; Wu et al.,
66 2013a, 2013b; Wu et al., 2011). Furthermore, hygroscopic growth is strongly influenced by
67 relative humidity (RH), which also varies greatly in space and time (Köppen, 1900; Dai, 2006;
68 Willett et al., 2014). Measurements made in different seasons and locations may suffer the cut-
69 off shift to different extents. Without sufficient understanding of the cut-off shift, it is difficult
70 to derive consistent seasonal variations and yearly trends of particle composition or compare
71 different locations. Moreover, insufficient knowledge of the cut-off shift can hinder effective
72 model validation. Most modelling results provide the mass loading and chemical composition
73 of dry particles (e.g., Archer-Nicholls et al., 2015; Mann et al., 2014; Mann et al., 2010; Tsyro,
74 2005; Zaveri et al., 2008), but filter measurements report results under ambient RH (i.e., wet
75 particles). The impact of this on model validation is expected to be important over humid

76 regions, e.g. marine and coastal regions where high RH and abundant hygroscopic sea-salt
77 particles are both present (Chen et al., 2016; Neumann et al., 2016a, 2016b).

78 Despite the important influence of hygroscopic growth and cut-off shift on particle composition
79 and loading measurements, there is no efficient way to dry the airflow for a high-volume
80 aerosol sampler. The airflow better not be heated or dried during the sampling, since these
81 processes change the gas-particle equilibrium and lead to a loss of semi-volatile compounds
82 (Chow, 1995; Grassian, 2001; Mader & Pankow, 2001; Schaap et al., 2011; Van Dingenen et
83 al., 2004; Shingler, et al., 2016;), e.g. nitrate (Chow et al., 2005; Hering & Cass, 1999; Schaap
84 et al., 2004; Slanina et al., 2001; Vecchi et al., 2009; Chen et al., 2018) and secondary organic
85 aerosols (Iinuma et al., 2010; Mader & Pankow, 2000). As recommended by EPA and
86 WMO/GAW (EPA, 1999; WMO/GAW, 2016), the inlet should sample the particles under
87 ambient conditions. It is worth noting that some experiments dry airflow in inlet manifolds due
88 to different scientific focuses, this would lead to evaporative losses of semi-volatile compounds
89 and Shingler et al. (2016) estimated the losses based on thermo-kinetic simulations.
90 Consequently, the influence due to cut-off shift is inherent in measurements of particle
91 composition, and requires full investigation and careful assessment to ensure consistent
92 comparisons between measurements.

93 In this study, we propose a method to assess the influence of this cut-off shift on particle
94 composition and loading measured using filter-based sampling. A global perspective on the
95 influence is presented first, based on κ -Köhler theory (which describes the hygroscopic growth
96 of particles, Köhler, 1936; Petters & Kreidenweis, 2007) together with previously reported
97 annual climatological values of hygroscopic properties, meteorological parameters (RH and
98 temperature) and particle volume size distributions. This work enables us to quantify the
99 influence of cut-off shift on analysis of particulate matter loading and composition, provides a
100 firm foundation for more consistent studies of the long-term characteristics and spatial
101 distributions, and brings more confidence to model validation.

102 **2. Method and Data**

103 To explore the influence of cut-off shift on filter-based particle sampling driven by hygroscopic
104 growth, we calculate the aerodynamic diameter of ambient particles based on the hygroscopic
105 diameter growth factor (GF). The GFs are derived from κ -Köhler theory (Petters &
106 Kreidenweis, 2007), with consideration of particle composition and size as well as

107 meteorological conditions (Eq. 1). In this study, particles are assumed to be homogeneously
 108 internally mixed with the same chemical constitution throughout each size mode, and the
 109 influence of the cut-off shift on total particulate matter loading is assessed. The influence on
 110 each particle component can also be assessed, although there is uncertainty resulting from the
 111 assumption about the particle mixing state (discussed in the section 3.3). More precise
 112 assessment of the influence of cut-off shift on particle components can be derived using the
 113 approach we propose here if detailed observations of particle mixing state and size-segregated
 114 composition are available. The collection efficiency, which depends on aerodynamic design of
 115 the impactor, air flow rate and pressure drop (Hillamo & Kauppinen, 1991; Marple et al., 1991;
 116 Wang & John, 1988), influences the sampled particles. This will influence the cut-off shift,
 117 which is generally less than 10% and is discussed in detail in section 3.4. In this study, we
 118 assume that the influence of sampling collection efficiency is corrected during chemical post-
 119 processing, so that particles larger than the nominal cut-off thresholds are totally blocked by
 120 the impactor and are not collected on the filter.

121 The κ -Köhler theory proposes a single parameter (κ) to describe the hygroscopic properties of
 122 particles, representing the dependence of hygroscopicity on chemical composition. The
 123 original Köhler equation (Köhler, 1936) can be transformed into the following Eq. (1), which
 124 describes the relationship between RH, κ and dry particle diameter (Liu et al., 2014; Petters &
 125 Kreidenweis, 2007):

$$RH/100 = \frac{GF^3 - 1}{GF^3 - 1 + \kappa} \exp\left(\frac{4\sigma_{s/a}M_w}{R(T + 273.15)\rho_w D_{dry}GF}\right) \quad (1)$$

126 where RH has units of [%], GF is the diameter of an ambient particle divided by its dry diameter
 127 (D_{dry} , [m]), T is the temperature [°C], $\sigma_{s/a}$ is the surface tension of the solution–air interface, R
 128 is the universal gas constant, M_w is the water molar weight, ρ_w is the water density, and κ is the
 129 hygroscopicity parameter. More details of the κ value and density of each components from
 130 previous studies are given in Table S1, please see also the references (Asa-Awuku et al., 2010;
 131 Bond & Bergstrom, 2006; Cross et al., 2007; Fountoukis & Nenes, 2007; Liu et al., 2014;
 132 McMeeking et al., 2010; Petters & Kreidenweis, 2007; Pringle et al., 2010).

133 The κ value of an internally mixed particle can be derived from its composition using the
 134 Zdanovskii-Stokes-Robinson (ZSR) mixing rule (Stokes & Robinson, 1966; Zdanovskii, 1948),
 135 which weights the κ of each component according to its respective volume fraction. A previous

136 modelling study (Pringle et al., 2010) provided the global distribution of κ for fine (0.1-1 μm)
137 particles, showing a fair agreement with most measurement-derived κ . The deviations between
138 the modelled and observed κ values were less than 0.05 at 10 out of the 14 locations (Pringle
139 et al., 2010). We adopt their statistical κ value for each continent in this study (Tables 1 and 2
140 in Pringle et al., 2010), and assume that the coarse particles (1-10 μm) have the same κ as fine
141 particles in the absence of size-resolved κ studies. The measured chemical properties or size-
142 resolved κ of particles is applied where available (Marine, Beijing and Melpitz cases described
143 below). O'Dowd et al. (2004) reported that coarse marine particles are very close to pure sea-
144 salt with more than 90% sodium chloride, whereas fine marine particles consist of more organic
145 components. Therefore, κ of sodium chloride is adopted for coarse marine particles in this study;
146 while the κ of fine marine particles follows Pringle et al. (2010). Liu et al. (2014) investigated
147 the size-resolved κ based on chemical composition measurements at a background station on
148 the North China Plain (NCP) near Beijing. The HOPE-Melpitz campaign (part of the HD(CP)2
149 Observational Prototype Experiment, Macke et al., 2017) provided size-segregated (PM_{10} and
150 PM_{10}) chemical ions and composition from filter measurements with a high-volume DIGITEL
151 DHA-80 sampler (Walter Riemer Messtechnik, Germany), more details of sampling and
152 laboratory analysis are given elsewhere (Spindler et al., 2013; Spindler et al., 2004). The
153 ISORROPIA II thermodynamic model (Fountoukis & Nenes, 2007) is used to derive the
154 inorganic components (e.g. ammonium nitrate and ammonium sulfate, please see details in
155 Table S1 and Fountoukis & Nenes, 2007) from ions measured by filter sampling at Melpitz.
156 We then follow the approach proposed by Liu et al. (2014) to derive κ for fine and coarse
157 modes based on their chemical composition. Homogeneous mixing is assumed for all chemical
158 components in fine and coarse modes in the absence of size-resolved particle composition
159 information. Therefore, κ is different between fine and coarse modes, but is consistent within
160 each mode.

161 Dry particle volume size distributions (PVSD) can be described by a multimodal distribution,
162 namely a lognormal distribution in the fine/accumulation (0.1-1 μm) and coarse (> 1 μm) modes
163 (Whitby, 1978). In this study, we follow the typical PVSDs in different air-mass/aerosol-
164 type/site categories in Whitby (1978), which are based on a compilation of global in-situ
165 measurements. For a specific case at Melpitz, we derive the PVSD from measurements using
166 an Aerodynamic Particle Sizer (APS Model 3320, TSI, Inc., Shoreview, MN USA) and a Twin
167 Differential Mobility Particle Sizer (TDMPS, Birmili et al., 1999, TROPOS, Leipzig,
168 Germany). Both APS and TDMPS were operated under dry conditions, and measured particle

169 number size distribution in the coarse and fine modes, respectively. PVSD is then calculated
170 assuming a spherical shape. The mobility diameter is converted to an aerodynamic diameter
171 following Chen, et al. (2016) and Heintzenberg et al. (1998). It is worth noting that fine
172 particles also include the Aitken mode ($< 0.1 \mu\text{m}$), which is not considered in this study since
173 it is negligible for the mass/volume loading and too small to be cut off.

174 To estimate the hygroscopic growth and cut-off shift, we use the annual climatological global
175 distribution of surface RH reported by (Dai, 2006) for each continent and for marine regions.
176 This is based on an analysis of long-term (1976-2002) global measurements from over 15,000
177 weather stations and ships. A recent study (Willett et al., 2014) based on 1976-2005 global
178 measurements reported annual climatological surface temperatures (T) and RH, and shows a
179 good agreement with Dai (2006). The reported surface temperature is adopted for each
180 continent, and a fixed surface temperature of 26.85°C (300 K) is assumed over marine regions
181 due to absence of data. Although this does not provide a realistic T variation, GF is insensitive
182 to T in the range -30°C to $+30^\circ\text{C}$, and less than 5% difference is observed for a $1 \mu\text{m}$ sea-salt
183 particle when $\text{RH}=90\%$, according to κ -Köhler theory (Fig. S1). For specific cases in Beijing
184 (Liu et al., 2014) and Melpitz (September 2013), the average RH and T observed during the
185 corresponding sampling periods were used.

186 **3. Results and Discussion**

187 The cut-off shift due to aerosol hygroscopic growth is ubiquitous in particle composition
188 measurements made with filter-based sampling. Fig. 1 and Table S2 summarize the influences
189 of cut-off shift on particle sampling (PM_{10} , $\text{PM}_{2.5}$ and PM_{10}) for different site/aerosol-type
190 categories following the classification in Whitby (1978), including marine surface (sea-salt),
191 desert dust, tropical forest, urban-average, average background, clean continental background,
192 background and aged urban plume, as well as urban and freeway. These assessments are based
193 on annual climatological datasets, but it is worth noting that the cut-off shift can vary
194 substantially during different measurement periods. The resulting influence for a specific
195 observation can be assessed using the corresponding measurement data via this proposed
196 approach, as shown later for specific measurement campaigns in Beijing and Melpitz.

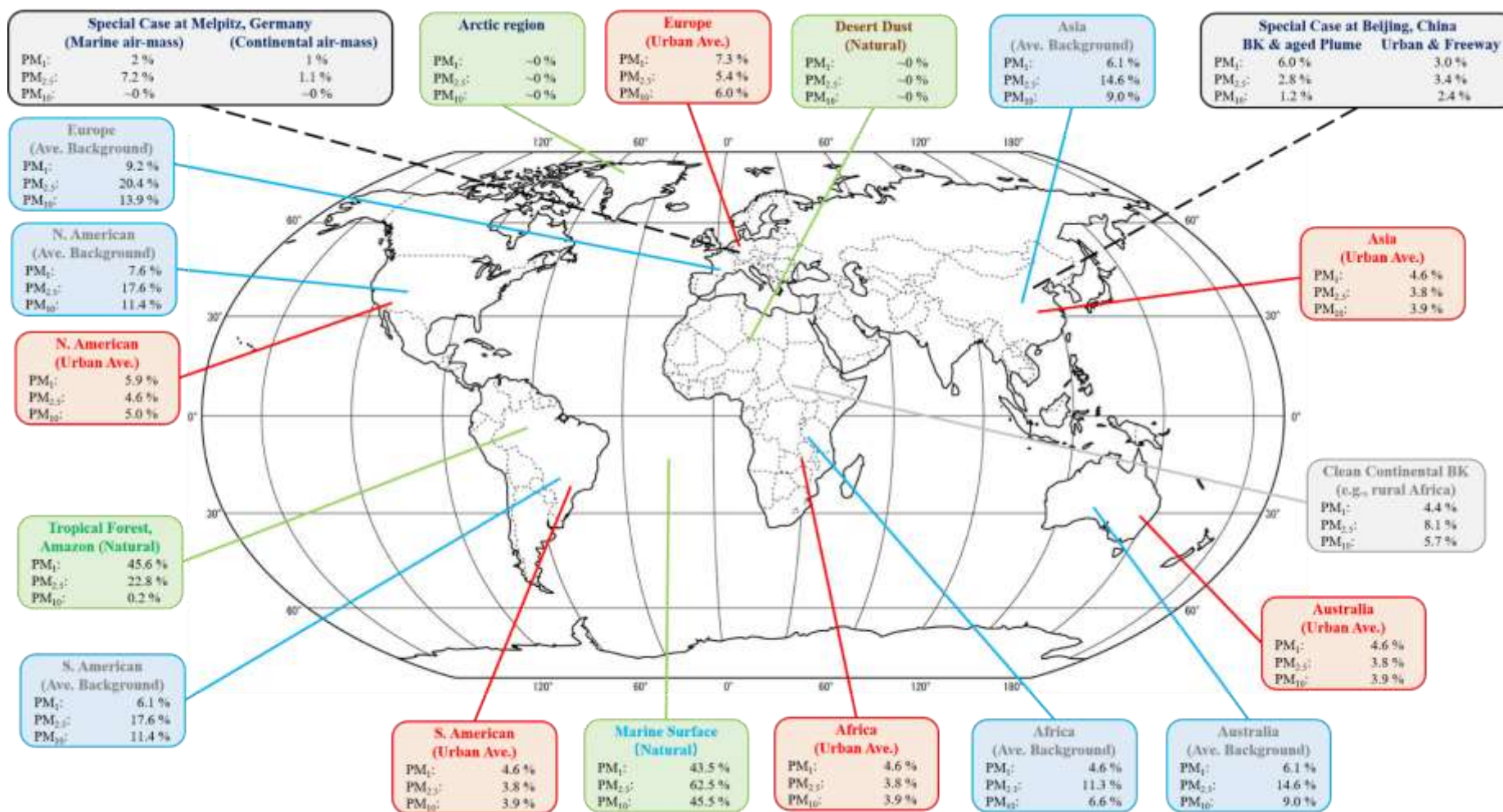


Figure 1. The influence of cut-off shift on particle mass loading. Green box (natural source aerosols), red box (urban-average over continents), blue box (average background over continents), grey box (clean continental background, taking Africa for example), and black box (two specific cases: Beijing & Melpitz). Annual climatological values are shown in this figure, more detailed parameters and uncertainties are given in Table S2 and S3.

198 3.1 Influences of the cut-off shift on particle measurements

199 Of particles from natural sources, sea-salt experiences the most significant influence of cut-off
200 shift, due to its high hygroscopicity (Twomey, 1954; Petters & Kreidenweis, 2007), high
201 volume/mass fraction at large sizes (Fig. S2), and high RH over marine surfaces (Dai, 2006).
202 As shown in Fig. 2, the influence on sampled sea-salt particles in PM_{2.5} can exceed 80% when
203 RH is higher than 90%. Over marine surfaces, as much as ~60% (median value) of sea-salt is
204 estimated to be additionally cut off by a PM_{2.5} impactor/inlet head compared with dry
205 conditions, and up to ~45% by a PM₁/PM₁₀ impactor (Table S2). In contrast, there is almost no
206 influence on hydrophobic dust particles (Pringle et al., 2010) and Arctic particles. Arctic
207 particles rarely reach sizes larger than 0.5 μm (Heintzenberg & Leck, 2012; Heintzenberg et
208 al., 2006; Korhonen et al., 2008), far below the cut off threshold. The influence on PM₁₀
209 sampling is negligible for biogenic particles over tropical regions, due to their low
210 hygroscopicity ($\kappa \sim 0.1$, (Pringle et al., 2010) and very limited volume/mass fraction around
211 10 μm (Huffman et al., 2012). However, the influence on tropical forest particles sampled by
212 PM₁ impactor can reach up to ~45%, and more than 20% by PM_{2.5} impactor. This is because
213 there is a large contribution from biogenic particles with sizes around 1 μm and 2.5 μm to the
214 total volume of PM₁ and PM_{2.5}, respectively (Huffman et al., 2012), see Fig. S2. Generally, the
215 influence of cut-off shift on filter-based sampling is negligible for dust, but should be
216 comprehensively considered for aerosols over marine and coastal regions, as well as tropical
217 forest. Greater care should be taken for a size-segregated particle composition analysis, where
218 the cut-off shift not only influences the total PM mass, but may also shift particles from smaller
219 size bins to larger bins.

220 Over regions influenced by anthropogenic activities, our estimated ALW is consistent with
221 previously reported values (Nguyen et al., 2016) all over the world. The highest contribution
222 of ALW (in percentage) to continental ambient total particle mass concentrations is found to
223 be in Europe. ALW contributes 22-56% (median 40%) of ambient total particle mass
224 concentrations in an urban-average air-mass over Europe (Table S2), but less than 30% over
225 other continents. This is because urban-average particles generally have a relatively low
226 hygroscopicity, with median κ values less than 0.3 on continents other than Europe, where a
227 higher median κ value of 0.36 (Pringle et al., 2010) and a relatively humid atmosphere (average
228 RH \sim 75%, Dai, 2006) are both present. In an extreme case with high RH and highly
229 hygroscopic particles present simultaneously, the contribution of ALW to the ambient total

230 particle mass concentrations may reach up to ~95% in a European average background air-
 231 mass, much higher than in an urban-average air-mass. In general, average background particles
 232 are larger than urban-average particles (Whitby, 1978), resulting in a reduction of the Kelvin
 233 effect and therefore an enhancement in water vapour condensation and cut-off shift.
 234 Correspondingly, the median value of the resulting influences on PM₁/PM_{2.5}/PM₁₀ sampling
 235 over European cities (urban-average sites) can be 5.5-7.5%, and may reach 50-60% (median
 236 value ~10-20%) for average background sites. Over other continents, the influence for urban
 237 sites is almost negligible (<5%), and for average background sites is about 10-17% for PM_{2.5}
 238 and less than 10% for PM₁ and PM₁₀. Taking rural regions in Africa as an example of clean
 239 continental background, the influence is ~5% for PM₁ and PM₁₀ measurements and ~8% for
 240 PM_{2.5} measurements. Reported measurements over the NCP/Beijing region in summer 2007
 241 are adopted in this study as examples of ‘background and aged urban plume’ and ‘urban and
 242 freeway’ (Liu et al., 2014), and the influences are found to be negligible (<6%) for PM₁, PM_{2.5},
 243 and PM₁₀ here.

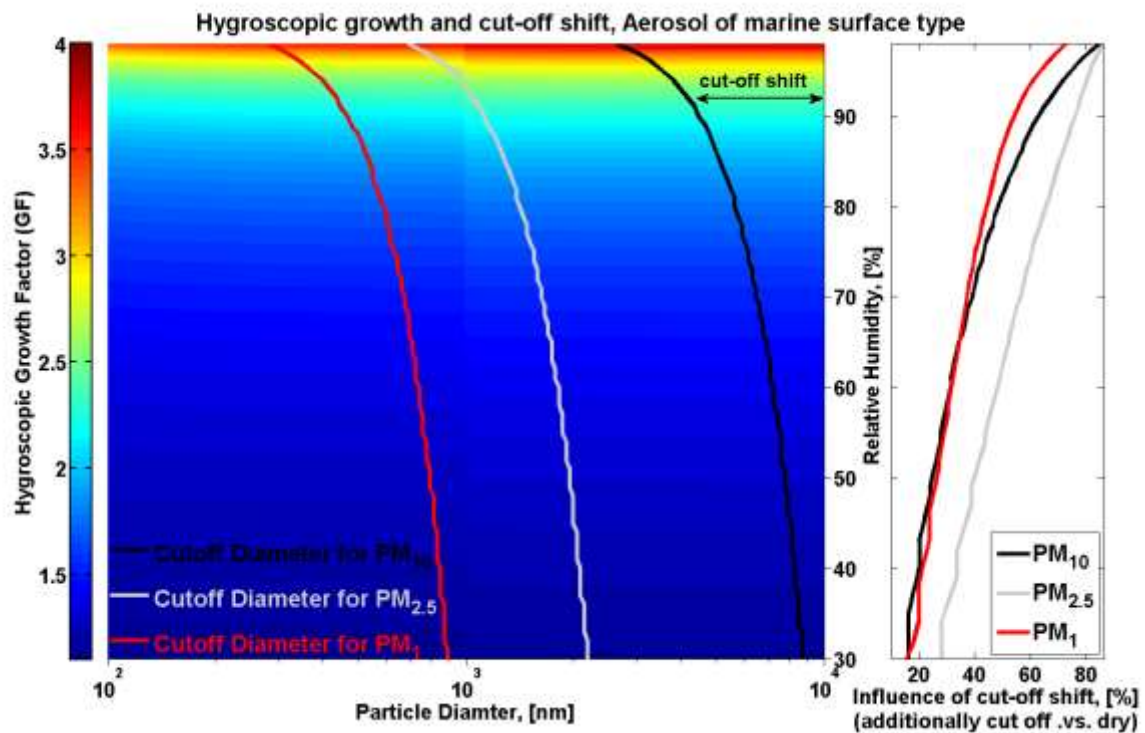


Figure 2. The hygroscopic diameter growth factor (GF, left panel) of marine surface aerosol, including fine mode (considerable organic components) and coarse mode (nearly pure sea salt), under different RH condition. The cut-off point of dry particles under different RH condition is indicated by the colourful lines (red: PM₁; grey: PM_{2.5}; black: PM₁₀). The influences of cut-off shift on particle volume concentrations are given in the right panel.

244

245 **3.2 Variability of the cut-off shift**

246 The influence of the cut-off shift varies greatly with time as well as location. Understanding
247 this variability is critical for study of the long-term and spatial distribution of particle
248 composition and for model validation. Observational data from the HOPE-Melpitz campaign
249 are used to illustrate this variability. Generally, the influence is small (<10%) at Melpitz, a
250 central European background site, where the coarse particle volume concentration is very
251 limited during this campaign (Fig. S3). However, the influence rapidly increased from ~1% to
252 ~7% for PM_{2.5} measurements (Fig. 1) when a marine air-mass brought hygroscopic coarse
253 particles to Melpitz (Fig. S3 and Fig. S4). Super-micron (1-2.5 μm) sea-salt particles
254 experienced substantial hygroscopic growth, and were strongly influenced by the cut-off shift.
255 This issue is of great importance for measurements at marine and coastal locations, where sea-
256 salt is an important contributor to total particulate matter. As shown in Fig. 2, there is a 30%
257 difference in the sampled sea-salt mass between RH=60% and RH=90% conditions due to the
258 cut-off shift alone.

259 **3.3 Impact of mixing state and aging process on cut-off shift**

260 The mixing state of particles can impact the cut-off shift. For instance, aging processes can mix
261 sea-salt with sulfate and organic carbon (OC) internally via heterogeneous reaction and
262 condensation, moderating the hygroscopic growth of sea-salt particle and influencing the cut-
263 off shift during sampling. Taking this aging process of sea-salt as an example, we conduct a
264 simplified theoretical investigation of the impact of mixing state on the cut-off shift. We make
265 the simplified assumptions that sea-salt is homogeneously internally mixed with more
266 hygroscopic sulfate (Na₂SO₄ with κ=0.76, Fountoukis & Nenes, 2007; Liu et al., 2014) and
267 less hygroscopic water soluble organic carbon (OC with κ=0.3, Asa-Awuku et al., 2011; Asa-
268 Awuku et al., 2010). A consistent percentage of sulfate and OC is assumed throughout all
269 particle sizes, and this percentage is used to indicate the extent of aging. We use the PVSD for
270 marine aerosol shown in Table S2, and assume that it remains unchanged during the aging
271 process. The Zdanovskii-Stokes-Robinson (ZSR) mixing rule is applied to calculate the κ
272 values of aged sea-salt-sulfate and sea-salt-OC particles, respectively. As shown in Fig. 3, the
273 influence of cut-off shift on the measured sea-salt mass loading decreases as aging increases.
274 This reduction in the influence is larger for PM₁₀/PM_{2.5} than PM₁ for sea-salt, and can decrease

275 by ~10% for sea-salt-sulfate and by 15-20% for sea-salt-OC particle once the aging level
 276 reaches 70%. The influence of cut-off shift reduces more slowly as RH falls. The influence of

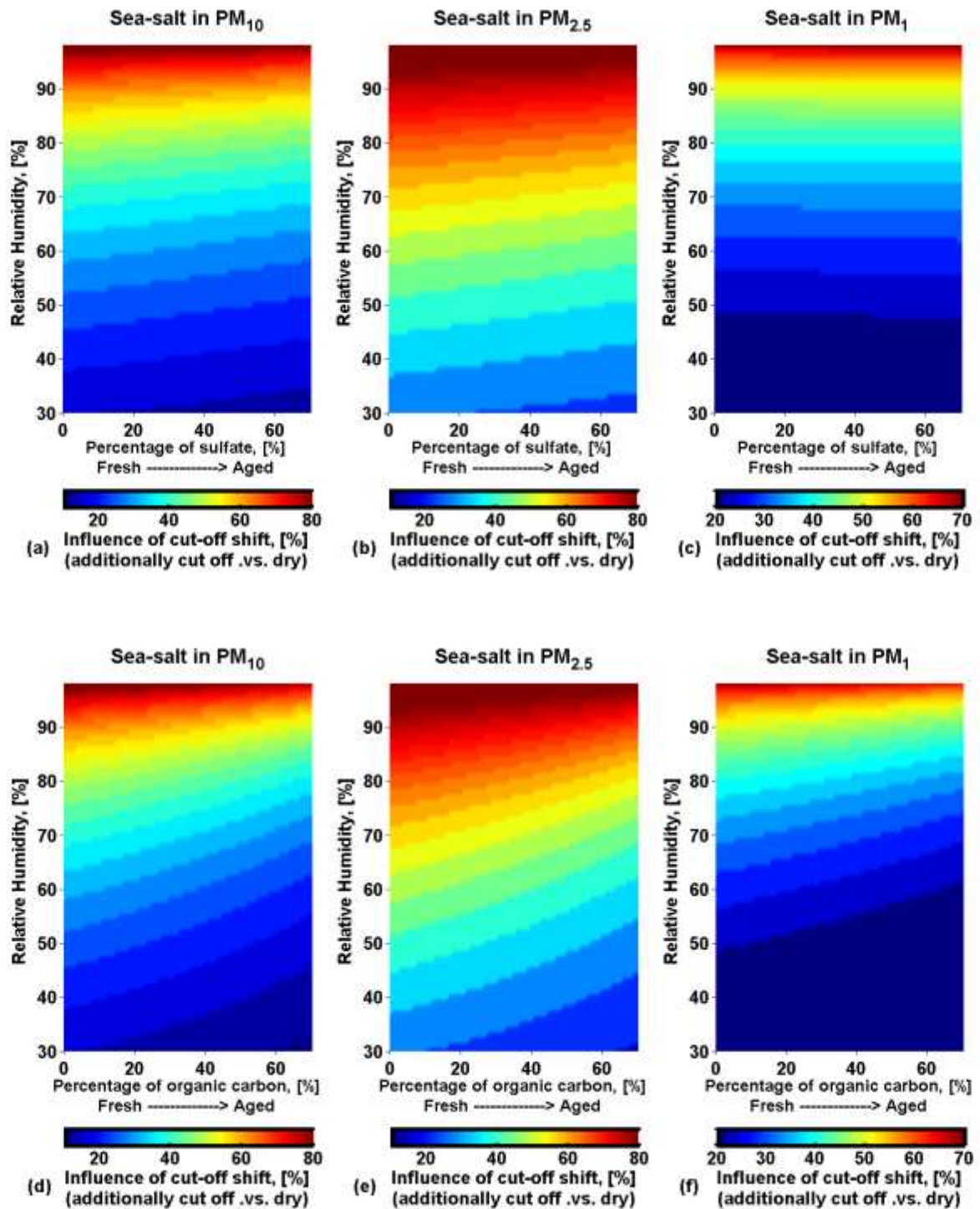


Figure 3. Impact of mixing state or aging process on the cut-off shift. (a, b, c) internally mixed between sea-salt and sulfate; (d, e, f) internally mixed between sea-salt and water soluble organic carbon. The percentage of sulfate or organic carbon indicates the aging level of sea-salt particles.

278

279 cut-off shift for sea-salt-OC particles is more sensitive to the aging level than sea-salt-sulfate
280 particles, due to the different hygroscopicity of sulfate and OC. Conversely, mixing with sea-
281 salt enhances the cut-off shift in measurements of sulfate and OC. For example, with RH=90%,
282 the influence of cut-off shift on sulfate measurements increases from 60% to 70% in PM₁₀ (70%
283 to 80% in PM_{2.5}) when the percentage of sea-salt increases from 30% to 80% (Fig. 3a and 3b).
284 Similarly, with RH=90%, the influence of cut-off shift on OC measurements increases from
285 55% to 70% in PM₁₀ (65% to 80% in PM_{2.5}) when the percentage of sea-salt increases from
286 30% to 80% (Fig. 3d and 3e). Detailed observations of mixing state are therefore needed in
287 future field measurements to refine assessment of the influence of cut-off shift on each particle
288 component.

289 **3.4 Impact of collection efficiency on cut-off shift**

290 The collection efficiency, depending on aerodynamic design of the impactor, air flow rate and
291 pressure drop influences the particle sampling. A ~2% over-sampling of sea-salt due to the
292 shallow collection efficiency curve (Fig. 4) is found, and this may decrease the influence of
293 cut-off shift. Here, we take the sampling of sea-salt particles with two PM₁₀ impactors as
294 examples to illustrate the impact of collection efficiency on cut-off shift. The PVSD of sea-salt
295 (Whitby, 1978) and collection efficiency curves of demonstrated impactors, TEOM PM₁₀ low
296 volume sampler (EPA, 1991) and impactor (Marple et al., 1991), are shown in Fig. 4. Taking
297 the collection efficiency curve into account, the influence of cut-off shift decreases slightly.
298 Generally, this impact of collection efficiency on cut-off shift increases slowly as RH increases;
299 however, as shown in Fig. 4, it remains less than 10% for the demonstrated shallow efficiency
300 curve (EPA, 1991) and less than 5% for the steep curve (Marple et al., 1991). This impact of
301 collection efficiency on cut-off shift is expected to be smaller on the PM₁/PM_{2.5} sampling of
302 sea-salt or sampling other types of aerosol. Since a single peak close to the cut-off threshold is
303 essential for a sensible impact of efficiency curve on particle sampling or cut-off shift. Dust
304 has a similar single peak PVSD to sea-salt, but it is hydrophobic and therefore there is no cut-
305 off shift due to hygroscopic growth.

306 **3.5 Impact of particle volume size distribution on the cut-off shift**

307 To investigate the impact of PVSD on the cut-off shift, we conduct sensitivity studies by
308 varying the geometric mean diameter by volume (D_{GV}), standard deviation (σ) and volume

309 concentration (V) of PVSD by $\pm 10\%$, as shown in Table S3. Two types of aerosol are chosen
 310 as examples. The first is marine surface aerosol, representing highly hygroscopic aerosol
 311 predominantly in the coarse mode; and the second is averaged urban aerosol in Asia,
 312 representing less hygroscopic aerosol with clearly defined fine and coarse modes in PVSD.
 313 Negligible impact ($< 2\%$) on the cut-off shift is observed for the second aerosol type due to its
 314 limited hygroscopicity. No impact from V can be observed for either aerosol type, since
 315 varying V does not change the shape of PVSD. Small differences (1-3%) in the influence of
 316 cut-off shift can be observed due to the variation of DGV in both aerosol types, although this
 317 effect could be larger in aerosols with a DGV lying close to the cut-off threshold of the impactor.
 318 However, a large impact can be observed for the highly hygroscopic marine aerosol with a $\pm 10\%$
 319 variation of σ . Although the differences for $PM_{2.5}$ and PM_{10} marine aerosol are generally
 320 smaller than 5%, an 8-14% difference in the influence of cut-off shift can be observed for PM_{10}
 321 marine aerosol when $RH=60\%$ (and 5-11% when $RH=90\%$). The particle size distribution is
 322 important for assessing the cut-off shift, and therefore it is very helpful if this can be measured
 323 during field campaigns.

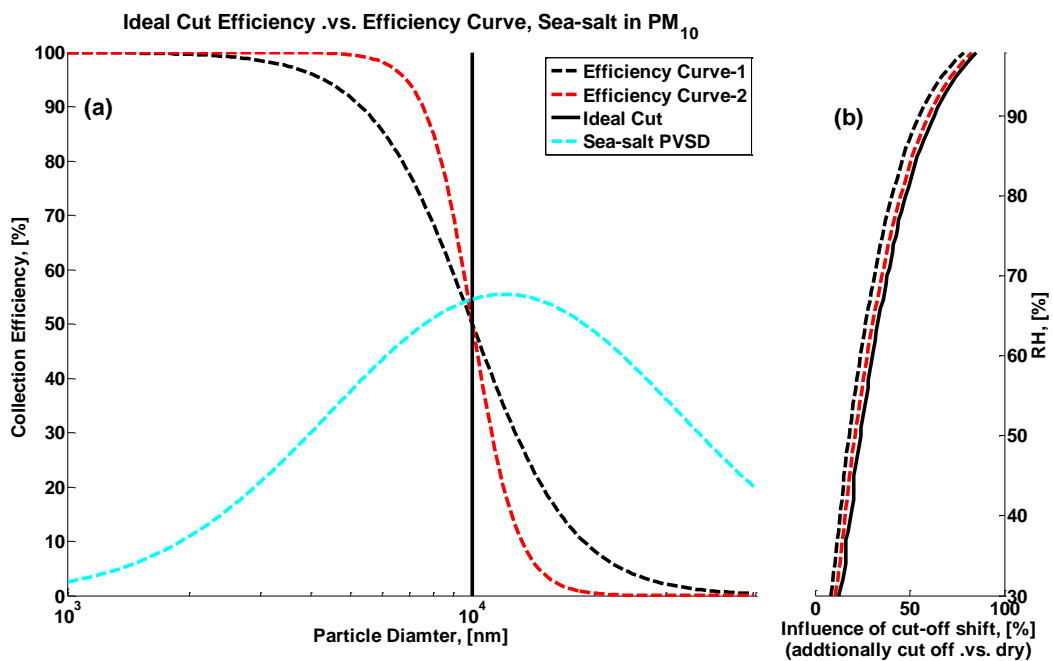


Figure 4. Impact of collection efficiency on cut-off shift during sea-salt sampling. Left panel (a) shows the PVSD (light blue dashed line) of sea-salt, an ideal efficiency curve (black solid line) and two collection efficiency curves of demonstrated impactors. The dashed black line indicates the TEOM PM_{10} low volume sampler (shallow curve, EPA, 1991); and the dashed red line indicates a steep-curve impactor (Marple et al., 1991). Right panel (b) shows the corresponding influences of

cut-off shift with consideration of two collection efficiency curves (dashed lines) and ideal cut (black solid line).

324 **4. Conclusions**

325 This study highlights the importance of the shift in the size of dry particles cut off by impactors,
326 resulting from hygroscopic growth. A method for assessing the influence of this cut-off shift
327 on analysis of particulate matter loading and composition is proposed, and an algorithm in
328 MATLAB language is provided in the supplementary materials. We present the first global
329 perspective of this influence.

330 Large temporal and spatial variation of the influence is found. On average, particles over
331 marine surfaces are found to experience the largest influence of cut-off shift, where as much as
332 ~60% of particle mass is estimated to be additionally cut off by a $PM_{2.5}$ impactor compared
333 with sampling under dry condition, and up to ~45% by a PM_1/PM_{10} impactor. In contrast, the
334 cut-off shift has no influence for dust and particles in the Arctic region. The influence for
335 biogenic particles in tropical forest is negligible for PM_{10} measurements, but considerable (23-
336 46%) for $PM_{2.5}$ and PM_1 measurements. The influence is generally negligible (less than 7%)
337 over urban areas, but need to be considered (about 10-20%) over continental background areas.
338 This influence needs to be assessed for each measurement period individually even at the same
339 location, since it is highly dependent on the ambient conditions. We estimate a difference of
340 ~30% in this influence of sea-salt particle sampling between relatively dry (RH=60%) and
341 humid (RH=90%) conditions. Our sensitivity studies show that detailed measurements of
342 particle size distribution and mixing state are helpful for refining assessments of this influence.

343 This work proposes a method to quantify the influence of cut-off shift on analysis of particulate
344 matter loading and composition, and to investigate the variability of this influence from a
345 temporal and spatial perspective. It is critical for observational studies focusing on long-term
346 and spatial distribution of particle loading and composition, and crucial for robust validation
347 of aerosol modules in modelling studies.

348

349 **Supplementary Materials**

350 Figure S1-S4;

351 Table S1-S3;

352 The MATLAB script in the '.m' files.

353

354

355 **Acknowledgments**

356 The HOPE campaign was funded by the German Research Ministry (grant number
357 01LK1212 C). The work of O. Wild and G. McFiggans was supported by the PROMOTE
358 project funded by NERC (NE/P016405/1 and NE/P016480/1). The work of Y. Chen was
359 supported by HOPE and PROMOTE. We thank Dr. Konrad Müller (TROPOS) for his
360 contribution to size-segregated particulate compositions measurements.

361

362

363 **References:**

364 IPCC, 2013. Climate Change 2013: The Physical Science Basis. Contribution of Working
365 Group I to the Fifth Assessment Report of the Intergovernmental Panel on Climate
366 Change, Report, edited by: Stocker, T. F., Qin D. H., Plattner, G. K., Tignor, M. M. B.,
367 Allen, S. K., Boschung, J., Nauels, A., Xia, Y., Bex, V., and Midgley, P. M.,
368 Cambridge University Press, New York, *available at: <http://www.ipcc.ch/report/ar5>*
369 (*last access: 10 September, 2017*).

370 Archer-Nicholls, S., Lowe, D., Darbyshire, E., Morgan, W.T., Bela, M.M., Pereira, G.,
371 Trembath, J., Kaiser, J.W., Longo, K.M., Freitas, S.R., Coe, H., McFiggans, G., 2015.
372 Characterising Brazilian biomass burning emissions using WRF-Chem with MOSAIC
373 sectional aerosol. *Geosci. Model Dev.* 8, 549-577.

374 Asa-Awuku, A., Moore, R.H., Nenes, A., Bahreini, R., Holloway, J.S., Brock, C.A.,
375 Middlebrook, A.M., Ryerson, T.B., Jimenez, J.L., DeCarlo, P.F., Hecobian, A., Weber,
376 R.J., Stickel, R., Tanner, D.J., Huey, L.G., 2011. Airborne cloud condensation nuclei
377 measurements during the 2006 Texas Air Quality Study. *Journal of Geophysical*
378 *Research: Atmospheres* 116, D11201.

379 Asa-Awuku, A., Nenes, A., Gao, S., Flagan, R.C., Seinfeld, J.H., 2010. Water-soluble SOA
380 from Alkene ozonolysis: composition and droplet activation kinetics inferences from
381 analysis of CCN activity. *Atmos. Chem. Phys.* 10, 1585-1597.

382 Aufschnaiter, T., 2009. DIGITEL High Volume Aerosol Sampler. Manual Version Hxx.38.

383 Berner, A., Luerzer, C., 1980. Mass size distributions of traffic aerosols at Vienna. The Journal
384 of Physical Chemistry 84, 2079-2083.

385 Birmili, W., Stratmann, F., Wiedensohler, A., 1999. Design of a DMA-based size spectrometer
386 for a large particle size range and stable operation. Journal of Aerosol Science 30, 549-
387 553.

388 Bond, T.C., Bergstrom, R.W., 2006. Light Absorption by Carbonaceous Particles: An
389 Investigative Review. Aerosol Science and Technology 40, 27-67.

390 Chen, Y., Cheng, Y., Ma, N., Wolke, R., Nordmann, S., Schüttauf, S., Ran, L., Wehner, B.,
391 Birmili, W., van der Gon, H.A.C.D., Mu, Q., Barthel, S., Spindler, G., Stieger, B.,
392 Müller, K., Zheng, G.J., Pöschl, U., Su, H., Wiedensohler, A., 2016a. Sea salt emission,
393 transport and influence on size-segregated nitrate simulation: a case study in
394 northwestern Europe by WRF-Chem. Atmos. Chem. Phys. 16, 12081-12097.

395 Chen, Y., Cheng, Y.F., Nordmann, S., Birmili, W., Denier van der Gon, H.A.C., Ma, N., Wolke,
396 R., Wehner, B., Sun, J., Spindler, G., Mu, Q., Pöschl, U., Su, H., Wiedensohler, A.,
397 2016b. Evaluation of the size segregation of elemental carbon (EC) emission in Europe:
398 influence on the simulation of EC long-range transportation. Atmos. Chem. Phys. 16,
399 1823-1835.

400 Chen, Y., Wolke, R., Ran, L., Birmili, W., Spindler, G., Schröder, W., Su, H., Cheng, Y., Tegen,
401 I., Wiedensohler, A., 2018. A parameterization of the heterogeneous hydrolysis of
402 N₂O₅ for mass-based aerosol models: improvement of particulate nitrate prediction.
403 Atmos. Chem. Phys. 18, 673-689.

404 Chow, J.C., 1995. Measurement Methods to Determine Compliance with Ambient Air Quality
405 Standards for Suspended Particles. Journal of the Air & Waste Management
406 Association 45, 320-382.

407 Chow, J.C., Watson, J.G., Lowenthal, D.H., Magliano, K.L., 2005. Loss of PM_{2.5} Nitrate from
408 Filter Samples in Central California. Journal of the Air & Waste Management
409 Association 55, 1158-1168.

410 Cross, E.S., Slowik, J.G., Davidovits, P., Allan, J.D., Worsnop, D.R., Jayne, J.T., Lewis †,
411 D.K., Canagaratna, M., Onasch, T.B., 2007. Laboratory and Ambient Particle Density
412 Determinations using Light Scattering in Conjunction with Aerosol Mass Spectrometry.
413 Aerosol Science and Technology 41, 343-359.

414 Dai, A., 2006. Recent Climatology, Variability, and Trends in Global Surface Humidity.
415 Journal of Climate 19, 3589-3606.

416 EPA, 1999. Particulate Matter (PM_{2.5}) Speciation Guidance, Final Draft, *available at:*
417 *https://www.epa.gov/ (last access: 18 September 2018).* EPA, 1991. Wind Tunnel Test
418 Report No. 29A: Test of the Rupprecht and Patashnick TEOM PM₁₀ Sampler Inlet at
419 2 and 24 KM/H, *available at: https://nepis.epa.gov/ (last access: 10 March, 2018).*

420 Fountoukis, C., Nenes, A., 2007. ISORROPIA II: a computationally efficient thermodynamic
421 equilibrium model for K⁺;Ca₂⁺;Mg₂⁺;NH₄⁺;Na⁺;SO₄²⁻;NO₃⁻;Cl⁻;H₂O aerosols. Atmos.
422 Chem. Phys. 7, 4639-4659.

423 Grassian, V.H., 2001. Heterogeneous uptake and reaction of nitrogen oxides and volatile
424 organic compounds on the surface of atmospheric particles including oxides,
425 carbonates, soot and mineral dust: Implications for the chemical balance of the
426 troposphere. *International Reviews in Physical Chemistry* 20, 467-548.

427 Heintzenberg, J., Leck, C., 2012. The summer aerosol in the central Arctic 1991–2008: did it
428 change or not? *Atmos. Chem. Phys.* 12, 3969-3983.

429 Heintzenberg, J., Leck, C., Birmili, W., Wehner, B., TjernstrÖM, M., Wiedensohler, A., 2006.
430 Aerosol number–size distributions during clear and fog periods in the summer high
431 Arctic: 1991, 1996 and 2001. *Tellus B* 58, 41-50.

432 Heintzenberg, J., Müller, K., Birmili, W., Spindler, G., Wiedensohler, A., 1998. Mass-related
433 aerosol properties over the Leipzig Basin. *Journal of Geophysical Research:*
434 *Atmospheres* 103, 13125-13135.

435 Heintzenberg, J., 1989. Fine particles in the global troposphere A review. *Tellus B: Chemical*
436 *and Physical Meteorology* 41, 149-160.

437 Hering, S., Cass, G., 1999. The Magnitude of Bias in the Measurement of PM₂₅ Arising from
438 Volatilization of Particulate Nitrate from Teflon Filters. *Journal of the Air & Waste*
439 *Management Association* 49, 725-733.

440 Hillamo, R.E., Kauppinen, E.I., 1991. On the Performance of the Berner Low Pressure
441 Impactor. *Aerosol Science and Technology* 14, 33-47.

442 Huffman, J.A., Sinha, B., Garland, R.M., Snee-Pollmann, A., Gunthe, S.S., Artaxo, P., Martin,
443 S.T., Andreae, M.O., Pöschl, U., 2012. Size distributions and temporal variations of
444 biological aerosol particles in the Amazon rainforest characterized by microscopy and
445 real-time UV-APS fluorescence techniques during AMAZE-08. *Atmos. Chem. Phys.*
446 12, 11997-12019.

447 Iinuma, Y., Böge, O., Gräfe, R., Herrmann, H., 2010. Methyl-Nitrocatechols: Atmospheric
448 Tracer Compounds for Biomass Burning Secondary Organic Aerosols. *Environmental*
449 *Science & Technology* 44, 8453-8459.

450 Köhler, H., 1936. The nucleus in and the growth of hygroscopic droplets. *Transactions of the*
451 *Faraday Society* 32, 1152-1161.

452 Köppen, W., 1900. Versuch einer Klassifikation der Klimate, vorzugsweise nach ihren
453 Beziehungen zur Pflanzenwelt. (Schluss). *Geographische Zeitschrift* 6, 657-679.

454 Korhonen, H., Carslaw, K.S., Spracklen, D.V., Ridley, D.A., Ström, J., 2008. A global model
455 study of processes controlling aerosol size distributions in the Arctic spring and summer.
456 *Journal of Geophysical Research: Atmospheres* 113, D08211.

457 Lee, Y.H., Adams, P.J., 2010. Evaluation of aerosol distributions in the GISS-TOMAS global
458 aerosol microphysics model with remote sensing observations. *Atmos. Chem. Phys.* 10,
459 2129-2144.

460 Liao, H., Seinfeld, J.H., 2005. Global impacts of gas-phase chemistry-aerosol interactions on
461 direct radiative forcing by anthropogenic aerosols and ozone. *Journal of Geophysical*
462 *Research: Atmospheres* 110, D18208.

463 Liu, H.J., Zhao, C.S., Nekat, B., Ma, N., Wiedensohler, A., van Pinxteren, D., Spindler, G.,
464 Müller, K., Herrmann, H., 2014. Aerosol hygroscopicity derived from size-segregated
465 chemical composition and its parameterization in the North China Plain. *Atmos. Chem.*
466 *Phys.* 14, 2525-2539.

467 Liu, P.F., Zhao, C.S., Göbel, T., Hallbauer, E., Nowak, A., Ran, L., Xu, W.Y., Deng, Z.Z., Ma,
468 N., Mildenberger, K., Henning, S., Stratmann, F., Wiedensohler, A., 2011. Hygroscopic
469 properties of aerosol particles at high relative humidity and their diurnal variations in
470 the North China Plain. *Atmos. Chem. Phys.* 11, 3479-3494.

471 Macke, A., Seifert, P., Baars, H., Barthlott, C., Beekmans, C., Behrendt, A., Bohn, B., Brueck,
472 M., Bühl, J., Crewell, S., Damian, T., Deneke, H., Düsing, S., Foth, A., Di Girolamo,
473 P., Hammann, E., Heinze, R., Hirsikko, A., Kalisch, J., Kalthoff, N., Kinne, S., Kohler,
474 M., Löhnert, U., Madhavan, B.L., Maurer, V., Muppa, S.K., Schween, J., Serikov, I.,
475 Siebert, H., Simmer, C., Späth, F., Steinke, S., Träumner, K., Trömel, S., Wehner, B.,
476 Wieser, A., Wulfmeyer, V., Xie, X., 2017. The HD(CP)2 Observational Prototype
477 Experiment (HOPE) – an overview. *Atmos. Chem. Phys.* 17, 4887-4914.

478 Mader, B.T., Pankow, J.F., 2000. Gas/solid partitioning of semivolatile organic compounds
479 (SOCs) to air filters. 1. Partitioning of polychlorinated dibenzodioxins, polychlorinated
480 dibenzofurans and polycyclic aromatic hydrocarbons to teflon membrane filters.
481 *Atmospheric Environment* 34, 4879-4887.

482 Mader, B.T., Pankow, J.F., 2001a. Gas/solid partitioning of semivolatile organic compounds
483 (SOCs) to air filters. 2. Partitioning of polychlorinated dibenzodioxins, polychlorinated
484 dibenzofurans, and polycyclic aromatic hydrocarbons to quartz fiber filters.
485 *Atmospheric Environment* 35, 1217-1223.

486 Mader, B.T., Pankow, J.F., 2001b. Gas/Solid Partitioning of Semivolatile Organic Compounds
487 (SOCs) to Air Filters. 3. An Analysis of Gas Adsorption Artifacts in Measurements of
488 Atmospheric SOCs and Organic Carbon (OC) When Using Teflon Membrane Filters
489 and Quartz Fiber Filters. *Environmental Science & Technology* 35, 3422-3432.

490 Mann, G.W., Carslaw, K.S., Reddington, C.L., Pringle, K.J., Schulz, M., Asmi, A., Spracklen,
491 D.V., Ridley, D.A., Woodhouse, M.T., Lee, L.A., Zhang, K., Ghan, S.J., Easter, R.C.,
492 Liu, X., Stier, P., Lee, Y.H., Adams, P.J., Tost, H., Lelieveld, J., Bauer, S.E., Tsigaridis,
493 K., van Noije, T.P.C., Strunk, A., Vignati, E., Bellouin, N., Dalvi, M., Johnson, C.E.,
494 Bergman, T., Kokkola, H., von Salzen, K., Yu, F., Luo, G., Petzold, A., Heintzenberg,
495 J., Clarke, A., Ogren, J.A., Gras, J., Baltensperger, U., Kaminski, U., Jennings, S.G.,
496 O'Dowd, C.D., Harrison, R.M., Beddows, D.C.S., Kulmala, M., Viisanen, Y., Ulevicius,
497 V., Mihalopoulos, N., Zdimal, V., Fiebig, M., Hansson, H.C., Swietlicki, E., Henzing,
498 J.S., 2014. Intercomparison and evaluation of global aerosol microphysical properties
499 among AeroCom models of a range of complexity. *Atmos. Chem. Phys.* 14, 4679-4713.

500 Mann, G.W., Carslaw, K.S., Spracklen, D.V., Ridley, D.A., Manktelow, P.T., Chipperfield,
501 M.P., Pickering, S.J., Johnson, C.E., 2010. Description and evaluation of GLOMAP-
502 mode: a modal global aerosol microphysics model for the UKCA composition-climate
503 model. *Geosci. Model Dev.* 3, 519-551.

504 Marple, V.A., Rubow, K.L., Behm, S.M., 1991. A Microorifice Uniform Deposit Impactor
505 (MOUDI): Description, Calibration, and Use. *Aerosol Science and Technology* 14,
506 434-446.

507 McMeeking, G.R., Hamburger, T., Liu, D., Flynn, M., Morgan, W.T., Northway, M.,
508 Highwood, E.J., Krejci, R., Allan, J.D., Minikin, A., Coe, H., 2010. Black carbon
509 measurements in the boundary layer over western and northern Europe. *Atmos. Chem.*
510 *Phys.* 10, 9393-9414.

511 Meister, K., Johansson, C., Forsberg, B., 2012. Estimated Short-Term Effects of Coarse
512 Particles on Daily Mortality in Stockholm, Sweden. *Environ. Health Persp.* 120, 431-
513 436.

514 Neumann, D., Matthias, V., Bieser, J., Aulinger, A., Quante, M., 2016a. A comparison of sea
515 salt emission parameterizations in northwestern Europe using a chemistry transport
516 model setup. *Atmos. Chem. Phys.* 16, 9905-9933.

517 Neumann, D., Matthias, V., Bieser, J., Aulinger, A., Quante, M., 2016b. Sensitivity of modeled
518 atmospheric nitrogen species and nitrogen deposition to variations in sea salt emissions
519 in the North Sea and Baltic Sea regions. *Atmos. Chem. Phys.* 16, 2921-2942.

520 Nguyen, T.K.V., Zhang, Q., Jimenez, J.L., Pike, M., Carlton, A.G., 2016. Liquid Water:
521 Ubiquitous Contributor to Aerosol Mass. *Environmental Science & Technology Letters*
522 3, 257-263.

523 O'Dowd, C.D., Facchini, M.C., Cavalli, F., Ceburnis, D., Mircea, M., Decesari, S., Fuzzi, S.,
524 Yoon, Y.J., Putaud, J.-P., 2004. Biogenically driven organic contribution to marine
525 aerosol. *Nature* 431, 676-680.

526 Petters, M.D., Kreidenweis, S.M., 2007. A single parameter representation of hygroscopic
527 growth and cloud condensation nucleus activity. *Atmos. Chem. Phys.* 7, 1961-1971.

528 Pope, C.A., Ezzati, M., Dockery, D.W., 2009. Fine-Particulate Air Pollution and Life
529 Expectancy in the United States. *New England Journal of Medicine* 360, 376-386.

530 Pringle, K.J., Tost, H., Pozzer, A., Pöschl, U., Lelieveld, J., 2010. Global distribution of the
531 effective aerosol hygroscopicity parameter for CCN activation. *Atmos. Chem. Phys.* 10,
532 5241-5255.

533 Putaud, J.-P., Raes, F., Van Dingenen, R., Brüggemann, E., Facchini, M.C., Decesari, S., Fuzzi,
534 S., Gehrig, R., Hüglin, C., Laj, P., Lorbeer, G., Maenhaut, W., Mihalopoulos, N., Müller,
535 K., Querol, X., Rodriguez, S., Schneider, J., Spindler, G., Brink, H.t., Tørseth, K.,
536 Wiedensohler, A., 2004. A European aerosol phenomenology—2: chemical
537 characteristics of particulate matter at kerbside, urban, rural and background sites in
538 Europe. *Atmospheric Environment* 38, 2579-2595.

- 539 Ramanathan, V., Carmichael, G., 2008. Global and regional climate changes due to black
540 carbon. *Nature geoscience* 1, 221-227.
- 541 Schaap, M., Otjes, R.P., Weijers, E.P., 2011. Illustrating the benefit of using hourly monitoring
542 data on secondary inorganic aerosol and its precursors for model evaluation. *Atmos.*
543 *Chem. Phys.* 11, 11041-11053.
- 544 Schaap, M., van Loon, M., ten Brink, H.M., Dentener, F.J., Builtjes, P.J.H., 2004. Secondary
545 inorganic aerosol simulations for Europe with special attention to nitrate. *Atmos. Chem.*
546 *Phys.* 4, 857-874.
- 547 Schauer, C., Niessner, R., Pöschl, U., 2003. Polycyclic Aromatic Hydrocarbons in Urban Air
548 Particulate Matter: Decadal and Seasonal Trends, Chemical Degradation, and
549 Sampling Artifacts. *Environmental Science & Technology* 37, 2861-2868.
- 550 Seinfeld, J.H., Pandis, S.N., 2006. *Atmospheric Chemistry and Physics: From Air Pollution to*
551 *Climate Change*. John Wiley & Sons, New York, 2nd Edn.
- 552 Shingler, T., Crosbie, E., Ortega, A., Shiraiwa, M., Zuend, A., Beyersdorf, A., Ziemba, L.,
553 Anderson, B., Thornhill, L., Perring, A.E., Schwarz, J.P., Campazano-Jost, P., Day,
554 D.A., Jimenez, J.L., Hair, J.W., Mikoviny, T., Wisthaler, A., Sorooshian, A., 2016.
555 Airborne characterization of subsaturated aerosol hygroscopicity and dry refractive
556 index from the surface to 6.5 km during the SEAC⁴RS campaign. *Journal of*
557 *Geophysical Research: Atmospheres* 121, 4188-4210.
- 558 Slanina, J., ten Brink, H.M., Otjes, R.P., Even, A., Jongejan, P., Khlystov, A., Waijers-Ijpelaan,
559 A., Hu, M., Lu, Y., 2001. The continuous analysis of nitrate and ammonium in aerosols
560 by the steam jet aerosol collector (SJAC): extension and validation of the methodology.
561 *Atmospheric Environment* 35, 2319-2330.
- 562 Spindler, G., Grüner, A., Müller, K., Schlimper, S., Herrmann, H., 2013. Long-term size-
563 segregated particle (PM₁₀, PM_{2.5}, PM₁) characterization study at Melpitz -- influence
564 of air mass inflow, weather conditions and season. *J Atmos Chem* 70, 165-195.
- 565 Spindler, G., Müller, K., Brüggemann, E., Gnauk, T., Herrmann, H., 2004. Long-term size-
566 segregated characterization of PM₁₀, PM_{2.5}, and PM₁ at the IfT research station
567 Melpitz downwind of Leipzig (Germany) using high and low-volume filter samplers.
568 *Atmospheric Environment* 38, 5333-5347.
- 569 Stokes, R.H., Robinson, R.A., 1966. Interactions in Aqueous Nonelectrolyte Solutions. I.
570 Solute-Solvent Equilibria. *The Journal of Physical Chemistry* 70, 2126-2131.
- 571 Tsyro, S.G., 2005. To what extent can aerosol water explain the discrepancy between model
572 calculated and gravimetric PM₁₀ and PM_{2.5}? *Atmos. Chem. Phys.* 5, 515-532.
- 573 Twomey, S., 1954. The Composition of Hygroscopic Particles in the Atmosphere. *Journal of*
574 *Meteorology* 11, 334-338. Van Dingenen, R., Raes, F., Putaud, J.-P., Baltensperger, U.,
575 Charron, A., Facchini, M.C., Decesari, S., Fuzzi, S., Gehrig, R., Hansson, H.-C.,
576 Harrison, R.M., Hüglin, C., Jones, A.M., Laj, P., Lorbeer, G., Maenhaut, W., Palmgren,
577 F., Querol, X., Rodriguez, S., Schneider, J., Brink, H.t., Tunved, P., Tørseth, K.,
578 Wehner, B., Weingartner, E., Wiedensohler, A., Wählin, P., 2004. A European aerosol

579 phenomenology—1: physical characteristics of particulate matter at kerbside, urban,
580 rural and background sites in Europe. *Atmospheric Environment* 38, 2561-2577.

581 Vecchi, R., Valli, G., Fermo, P., D'Alessandro, A., Piazzalunga, A., Bernardoni, V., 2009.
582 Organic and inorganic sampling artefacts assessment. *Atmospheric Environment* 43,
583 1713-1720.

584 Wang, H.-C., John, W., 1988. Characteristics of the Berner Impactor for Sampling Inorganic
585 Ions. *Aerosol Science and Technology* 8, 157-172.

586 Whitby, K.T., 1978. Proceedings of the International Symposium The physical characteristics
587 of sulfur aerosols. *Atmospheric Environment* 12, 135-159.

588 Willett, K.M., Dunn, R.J.H., Thorne, P.W., Bell, S., de Podesta, M., Parker, D.E., Jones, P.D.,
589 Williams Jr, C.N., 2014. HadISDH land surface multi-variable humidity and
590 temperature record for climate monitoring. *Clim. Past* 10, 1983-2006.

591 WMO/GAW, 2016. WMO/GAW Aerosol Measurement Procedures, Guidelines and
592 Recommendations. GAW Report No. 227, available at: <https://library.wmo.int/> (last
593 access: 18 September 2018).

594 Wu, Z.J., Birmili, W., Poulain, L., Wang, Z., Merkel, M., Fahlbusch, B., van Pinxteren, D.,
595 Herrmann, H., Wiedensohler, A., 2013a. Particle hygroscopicity during atmospheric
596 new particle formation events: implications for the chemical species contributing to
597 particle growth. *Atmos. Chem. Phys.* 13, 6637-6646.

598 Wu, Z.J., Poulain, L., Henning, S., Dieckmann, K., Birmili, W., Merkel, M., van Pinxteren, D.,
599 Spindler, G., Müller, K., Stratmann, F., Herrmann, H., Wiedensohler, A., 2013b.
600 Relating particle hygroscopicity and CCN activity to chemical composition during the
601 HCCT-2010 field campaign. *Atmos. Chem. Phys.* 13, 7983-7996.

602 Wu, Z.J., Nowak, A., Poulain, L., Herrmann, H., Wiedensohler, A., 2011. Hygroscopic
603 behavior of atmospherically relevant water-soluble carboxylic salts and their influence
604 on the water uptake of ammonium sulfate. *Atmos. Chem. Phys.* 11, 12617-12626.

605 Zaveri, R.A., Easter, R.C., Fast, J.D., Peters, L.K., 2008. Model for Simulating Aerosol
606 Interactions and Chemistry (MOSAIC). *Journal of Geophysical Research:*
607 *Atmospheres* 113.

608 Zdanovskii, A.B., 1948. Novyi Metod Rascheta Rastvorimostei Elektrolitov V
609 Mnogokomponentnykh Sistemakh .1. *Zhurnal Fizicheskoi Khimii* 22, 1478-1485.